

Nanomechanical Recognition of *N*-Methylammonium Salts

Marco Dionisio,[†] Giulio Oliviero,[‡] Daniela Menozzi,[†] Stefania Federici,[‡] Roger M. Yebeutchou,[†] Franz P. Schmidtchen,[§] Enrico Dalcanale,^{*,†} and Paolo Bergese^{*,‡}

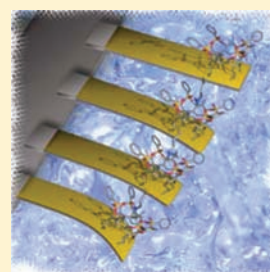
[†]Department of Organic and Industrial Chemistry, University of Parma, and INSTM, UdR Parma, Parco Area delle Scienze 17A, 43124 Parma, Italy

[‡]Chemistry for Technologies Laboratory, University of Brescia, Via Branze 38, 25123 Brescia, Italy

[§]Department Chemie, Technische Universität München, D-85747 Garching, Germany

Supporting Information

ABSTRACT: Turning molecular recognition into an effective mechanical response is critical for many applications ranging from molecular motors and responsive materials to sensors. Herein, we demonstrate how the energy of the molecular recognition between a supramolecular host and small alkylammonium salts can be harnessed to perform a nanomechanical task in a univocal way. Nanomechanical Si microcantilevers (MCs) functionalized by a film of tetra-phosphonate cavitands were employed to screen as guests the compounds of the butylammonium chloride series 1–4, which comprises a range of low molecular weight (LMW) molecules (molecular mass < 150 Da) that differ from each other by one or a few *N*-methyl groups (molecular mass 15 Da). The cavitand surface recognition of each individual guest drove a specific MC bending (from a few to several tens of nanometer), disclosing a direct, label-free, and real-time mean to sort them. The complexation preferences of tetraphosphonate cavitands toward ammonium chloride guests 1–4 were independently assessed by isothermal titration calorimetry. Both direct and displacement binding experiments concurred to define the following binding order in the alkylammonium series: 2 > 3 ≈ 1 ≫ 4. This trend is consistent with the number of interactions established by each guest with the host. The complementary ITC experiments showed that the host–guest complexation affinity in solution is transferred to the MC bending. These findings were benchmarked by implementing cavitand-functionalized MCs to discriminate sarcosine from glycine in water.



INTRODUCTION

Probing small molecules bearing amino-functionalities is a key issue from both the fundamental and the applied sides. *N*-Methylated moieties, in particular, are present in a broad range of biologically active compounds, from drugs¹ to cancer biomarkers² and neurotransmitters.³ These molecules are traditionally probed by liquid-and-gas-chromatography-based mass or light spectrometry⁴ or, limited to amphetamines and analogues, by label-based immunoassays and immunosensors.⁵ Label-free, direct, real-time, and in-fluid sensing remains highly desirable, but to date is severely hindered by the very low weight of the molecules, typically below 200 Da, that renders mass-based sensors, such as SPR (surface plasmon resonance) and QCM (quartz crystal microbalance), ineffective.⁶

We recently showed that the free energy released by a bimolecular ligand–receptor (viz. host–guest) interaction confined at a solid–solution interface splits into chemical and mechanical surface work, the latter determined by the work the host performs to “accommodate” the guest at the solid–solution interface.⁷ This work appears as a variation of the surface stress (surface pressure) and probes the recognition event in a label-free and energy-based fashion. Because it ranges from a few to several tens of mJ/m², surface work can be transduced/measured by the so-called mechanical biosensors,⁸ that include microcantilever (MC) beams⁹ and contact angle molecular recognition (CONAMORE) assays.¹⁰

Cantilever-based chemical sensors are limited, however, by the availability of coatings that interact exclusively and selectively with the analyte of interest. So far, for selective chemical and biological sensing, the choice of MC coating has been restricted to DNA or antibodies,^{9,11,12} neglecting the large pool of available synthetic receptors.

Phosphonate cavitands have established themselves as an outstanding, versatile class of synthetic receptors (hosts),¹³ whose molecular recognition properties have been exploited in gas sensing,¹⁴ supramolecular polymers,¹⁵ surface self-assembly,¹⁶ and product protection.¹⁷ Their ability to bind *N*-methylated ammonium salts via a synergistic mix of weak interactions such as H-bonding, dipole–dipole, and CH– π interactions has been already documented in the gas phase,¹⁸ in solution,¹⁹ and on surfaces.²⁰

The guest-induced modulation of these interactions across the alkylammonium salt series and their impact on the overall binding has not been studied so far.

In this Article, we present a fundamental study toward understanding the viability of nanomechanical sensors for probing small molecules bearing amino-functionalities. In particular, as sketched in Figure 1, we achieved label-free selective detection of *N*-methyl-ammonium salts in methanol

Received: November 10, 2011

Published: January 9, 2012

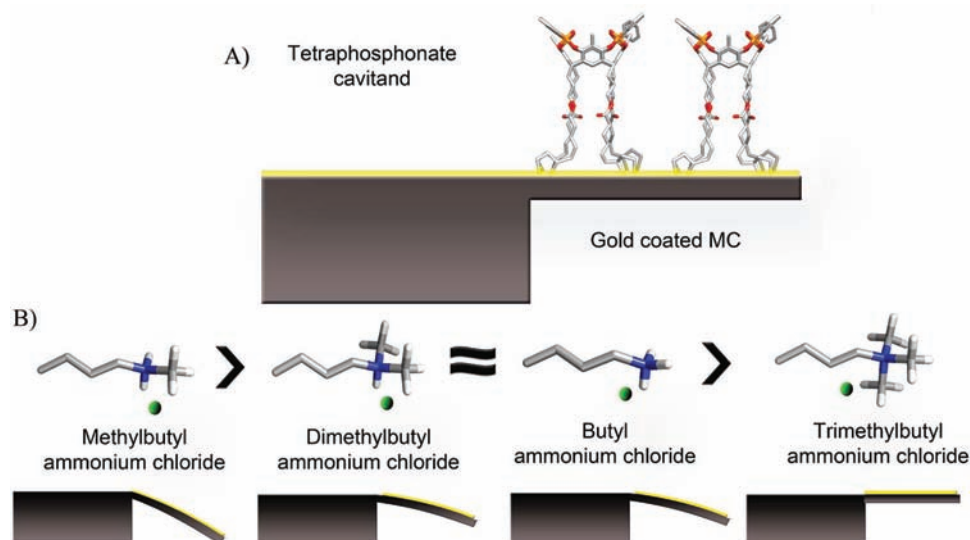


Figure 1. Working principle of the selective detection of *N*-methylammonium salts by cavita nd-functionalized MCs. (A) Si MCs ($500 \times 100 \times 1 \mu\text{m}^3$) with the top faces coated by a 20 nm Au are functionalized with a disulfide functionalized cavita nd. (B) The different binding energies of complexation of the active cavita nd with the different *N*-methyl-ammonium salts are mirrored by different variations of the surface stress that in turn are balanced by different MC deflections.

by MCs functionalized with tetraphosphonate cavita nds. These molecules are low molecular weight (LMW) species of a mass equal to or lower than 150 Da and that differ between each other only by a methyl group, which is 15 Da. Such unprecedented selectivity was attained thanks to the use of tetraphosphonate cavita nds as receptors (Figure 1). The observed complexation trend was independently confirmed and rationalized by isothermal titration calorimetry (ITC) measurements,²¹ performed both as direct titration and as displacement titration experiments.²²

Finally, the cavita nd functionalized MCs were benchmarked by detecting sarcosine in aqueous environment. This case of study is of topical interest in biomedical diagnostics, because sarcosine has been recently singled out as a possible early marker of the aggressive forms of prostate cancer.²

MATERIALS AND METHODS

Cavita nds and Guests. The compounds used in the present work are shown in Figure 2. The preparations of active cavita nds $\text{Tiii}[C_3H_7, CH_3, Ph]$ ¹⁸ and $\text{Tiii}[\text{disulfide}, CH_3, Ph]$ ²³ have already been described, while the synthesis of the reference cavita nd $\text{MeCav}[\text{disulfide}, CH_3]$ is reported in the Supporting Information. To be easily immobilized on MCs, $\text{Tiii}[\text{disulfide}, CH_3, Ph]$ and $\text{MeCav}[\text{disulfide}, CH_3]$ cavita nds were functionalized at the lower rim with four lipoic acid units. This allowed the cavita nd deposition on the top face of the MC with a stability comparable to thiols.²⁴

Guests 1–3 were prepared by protonation with HCl of the corresponding commercial amines, followed by crystallization from diethyl ether. Guest 4 was prepared via methylation of *N,N*-dimethylbutylamine with methyl iodide, followed by anion exchange with Dowex 22 chloride form (see the Supporting Information).

MC Experiments. Arrays of eight rectangular silicon MCs ($500 \times 100 \times 1 \mu\text{m}^3$) with the top faces coated by a 20 nm Au thin film were employed (Concentris GmbH, Basel, CH). The arrays were cleaned with acetone and ozone-UV before functionalization with the cavita nd. Each MC was then incubated for 3 h in a 1×10^{-5} M dichloroethane solution of the cavita nd by means of microcapillaries managed with the Cantisens Functionalization Unit (Concentris GmbH, Basel, CH). Following this procedure, MC arrays functionalized with the active $\text{Tiii}[\text{disulfide}, CH_3, Ph]$ and the control $\text{MeCav}[\text{disulfide}, CH_3]$ cavita nds were prepared.

Molecular recognition experiments were conducted by the Cantisens Research MC platform (Concentris GmbH, Basel, CH), which, in particular, is equipped with a microfluidic system to handle liquid delivery to the MCs and multiple lasers for simultaneous measurement of the deflection of the individual MCs. All experiments were conducted at $0.83 \mu\text{L/s}$ liquid flux. MC arrays were allowed to stabilize under pure methanol for about 20 min before the injection of the methylammonium salt (guest). After injection, the guest was allowed to flow in the measurement chamber for about 1.5 min (injection time frame), and then the pure methanol flux was restored again. MC deflections were tracked against time during all of these steps. Following this procedure, all guests at identical concentrations (1×10^{-5} M) were scanned against active as well as control MC arrays. The same experimental procedure for the MC molecular recognition tests was employed for the detection of sarcosine against glycine. In particular, Milli-Q water was employed as flowing liquid, and sarcosine and glycine were diluted in water to reach a molar concentration of 1×10^{-4} M. Both of the molecules were then tested on arrays functionalized with the active cavita nds.

ITC Experiments. ITC experiments were performed with an ITC-MCS calorimeter by MicroCal (GE Healthcare) at the temperature of 303 K and room pressure. The solutions were prepared in dry methanol (carefully degassed prior to use).

Direct titration experiments were performed by injecting 2–10 μL aliquots of the guest into a 10-fold lower concentrated cavita nd $\text{Tiii}[C_3H_7, CH_3, Ph]$ solution hosted in the reaction cell (cell volume = 1.35 mL) and the heat released upon binding tracked against time. To account for unspecific heats of dilution, each guest was also titrated into pure methanol (blank titration). In all cases, the signal from blank titrations was negligible with respect to the binding signal. Each experiment was replicated at least three times.

Displacement titration experiments consisted in the titration of the weaker guest into the host solution and the consecutive titration of the stronger guest in the obtained solution (displacement titration). Both of the titrations were conducted following the protocols given above for the direct binding experiments. The displacement experiments were counterchecked by directly titrating the weakest guest into the solution of the corresponding strongest complex.

RESULTS AND DISCUSSION

MC Experiments. Arrays of eight gold coated MCs, functionalized with $\text{Tiii}[\text{disulfide}, CH_3, Ph]$, were exposed

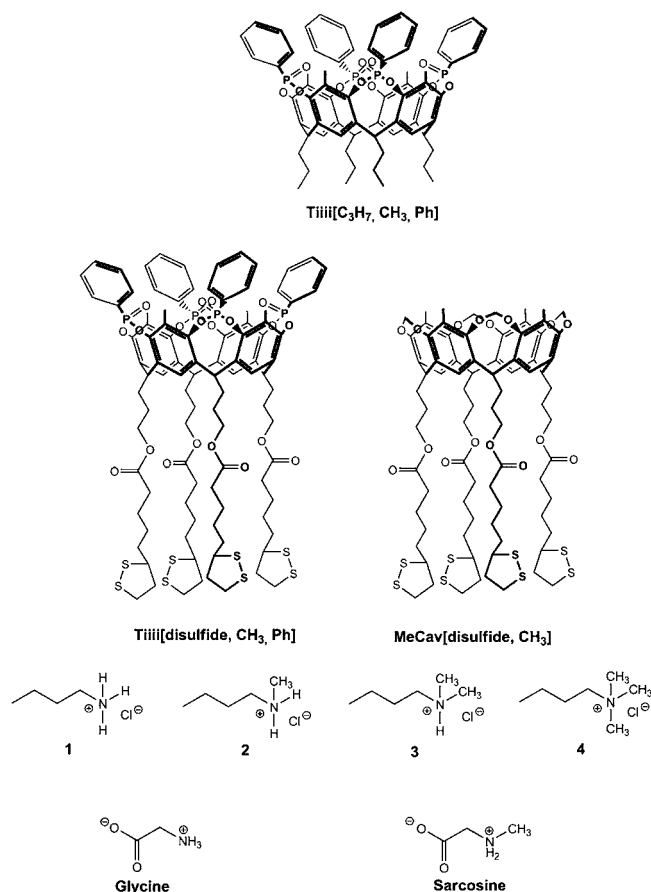


Figure 2. Scheme of the molecular structure of the cavitands and of the guests. $\text{Tiiii}[\text{C}_3\text{H}_7, \text{CH}_3, \text{Ph}]$ is the cavitant used for the ITC experiments, and $\text{Tiiii}[\text{disulfide}, \text{CH}_3, \text{Ph}]$ and $\text{MeCav}[\text{disulfide}, \text{CH}_3]$ are the active and the reference cavitands functionalized at the lower rim with lipoic groups, used for the MC experiments. The six guests are butylammonium chloride (1), *N*-methylbutylammonium chloride (2), *N,N*-dimethylbutylammonium chloride (3), *N,N,N*-trimethylbutylammonium chloride (4), glycine, and sarcosine zwitterions.

to a methanol solution of the four chosen guests at a molar concentration of 1×10^{-5} M. The mean signal of the eight MCs was monitored during the flow of each guest through the microfluidic chamber.

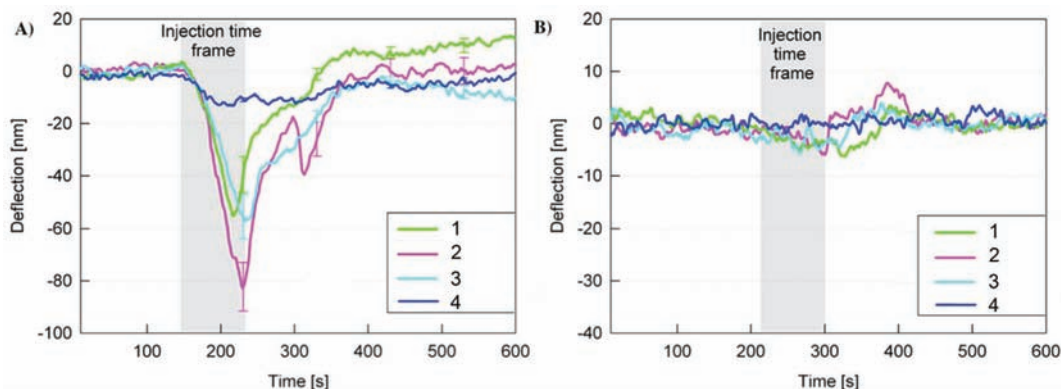


Figure 3. MC absolute deflections during the injection of a 1×10^{-5} M methanol solution of methyl-ammonium guests (gray area). Each line represents the mean deflection of the eight MCs, and the error bars are the SD of the mean at selected points. (A) MCs functionalized with the active cavitant $\text{Tiiii}[\text{disulfide}, \text{CH}_3, \text{Ph}]$. (B) MCs functionalized with the control cavitant $\text{MeCav}[\text{disulfide}, \text{CH}_3]$.

To rule out nonspecific responses due to physisorption, the MC bending should be referred to a reference MC. In view of this, we synthesized the control cavitant $\text{MeCav}[\text{disulfide}, \text{CH}_3]$, which is structurally similar to the active one. The active and control cavitands $\text{Tiiii}[\text{disulfide}, \text{CH}_3, \text{Ph}]$ and $\text{MeCav}[\text{disulfide}, \text{CH}_3]$ (Figure 2) differ only for the upper rim bridging group. The active one is a tetraphosphonate cavitant able to recognize the *N*-methylammonium salts after establishing H-bonding, dipole–dipole, and $\text{CH}-\pi$ interactions, while in the control one the $\text{P}=\text{O}$ units are substituted by methylene groups as the bridging groups. In the absence of the $\text{P}=\text{O}$ bridges, no recognition toward the *N*-methylammonium salt series was observed.²⁵

Figure 3A shows the four deflection signals for guests 1–4 obtained by monitoring the mean deflection of the eight MCs of an array functionalized with $\text{Tiiii}[\text{disulfide}, \text{CH}_3, \text{Ph}]$ while flowing the guest solutions into the chamber. In the selected reference system, a positive deflection ($\Delta z > 0$) corresponds to the upward bending of the cantilever due to tensile surface stress (with respect to the cantilever top face), and a negative deflection ($\Delta z < 0$) to a downward bending of the cantilever due to compressive surface stress. As it has been explained in the previous section, the guests were allowed to flow in the measurement chamber for about 90 s (injection time frame) after the injection, and then the pure methanol flux was restored again. The deflection curves perfectly match this timing; in fact, the binding kinetic reaches a maximum deflection 90 s after the guest entrance into the chamber, and then the release kinetics takes place. The curves show a deflection of -80 nm when guest 2 is introduced in the chamber, while a deflection of -50 nm occurs when guests 1 and 3 are injected. Guest 4 induces the lowest deflection with respect to the other three guests. As it is shown by the curves, the deflection signal reaches a peak, but not an equilibrium value, and the release kinetics seems to happen in two steps. The two-step release is clear in the guest 2 trace, while in the other three it is barely visible. This two-step release was observed for all of the performed static experiments, and it is possibly generated by interactions between the injected guests and the cavitands also during the release period. On the other hand, because the guests are very likely progressively swept out from the host cavities by the incoming solvent molecules, the way a new host–guest interaction would occur in the time

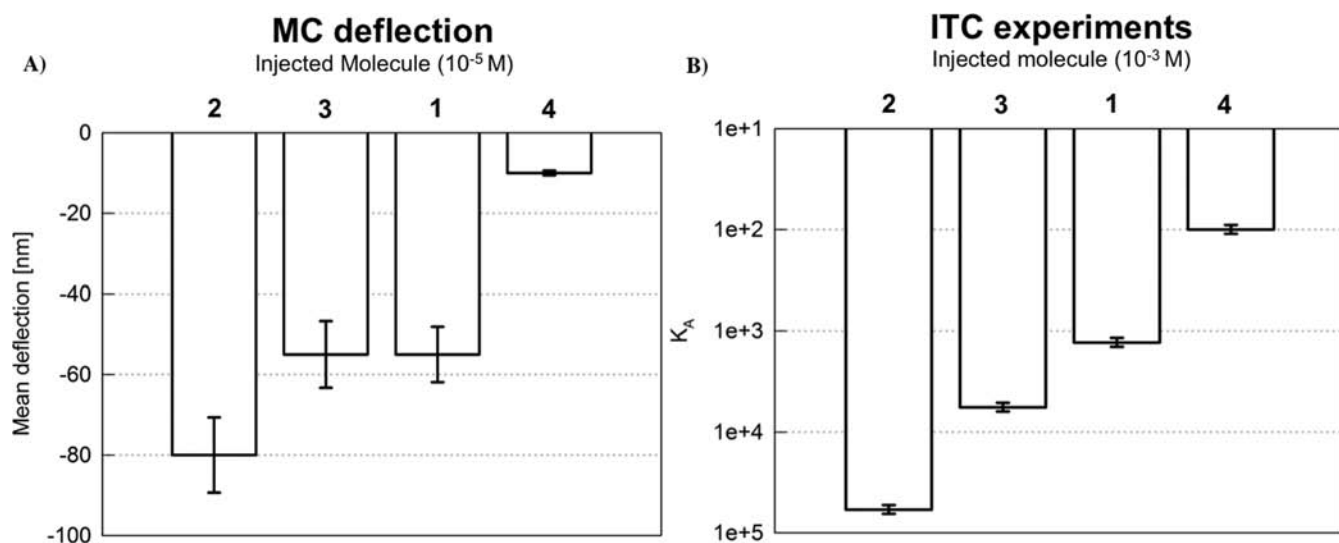


Figure 4. (A) Bar chart of MC deflections, the mean value, and the SD of the mean refer to four replicates. (B) Bar chart of the K evaluated by ITC, the mean value, and the SD of the mean refer to three replicates.

delay of the experiment is an open question. Work is in progress to clarify this issue.

Figure 3B displays the signal obtained by monitoring the mean deflection of the eight MCs of an array functionalized with the reference cavitant **MeCav[disulfide, CH₃]**. The deflection remains unchanged after the injection of each of the four guests (injections were conducted under the same conditions of the experiments with the active cavitant **Tiii[disulfide, CH₃, Ph]**).

The absence of responses supports the choice of the reference cavitant and implies that the deflection responses of the active cavitant MCs reported in Figure 3A are due only to the specific interactions between the host and the guests and rules out any unspecific event.

The obtained results were statistically validated by replicating the same series of experiments on four different arrays of eight MCs functionalized with the active cavitant **Tiii[disulfide, CH₃, Ph]**. The mean value of the deflection peaks of the four arrays and the error, intended as the overall standard deviation of the mean, are shown in the bar chart reported in Figure 4A. The trend of the interaction intensities indicated in Figure 3A is confirmed: the highest response is obtained when *N*-methylbutyl-ammonium chloride **2** is injected ($\overline{\Delta z} = (-80 \pm 10)$ nm), a comparable deflection is measured when salts **1** and **3** are in the chamber ($\overline{\Delta z} = (-55 \pm 6)$ nm), and the weakest response comes from salt **4** ($\overline{\Delta z} = (-10 \pm 2)$ nm).

These data, to the best of our knowledge, are the first that report statistically validated label-free recognition of LMW molecules. The cavitant functionalized MCs allow for detection and discrimination of guest molecules that weigh from 109 to 152 Da and differ between each other for one or more methyl groups (15 Da each) only.

Deflection results can be addressed in terms of the applied surface stress (σ) triggered by the host–guest complexation. The relation between the variation of the surface stress ($\Delta\sigma$) applied along the MC top face and its resulting deflection is given by Stoney's equation:

$$\Delta\sigma = \frac{1}{4s} \frac{\Delta z E t^2}{L^2(1-\nu)} \quad (1)$$

where Δz is the MC deflection, E is the MC Young's modulus, t is the MC thickness, L is the MC length, ν is the MC Poisson's ratio, and s is the Sader correction factor.²⁶ $\Delta\sigma$ is related to the properties of the stress inducer, whose role in our case is played by the host–guest complexation confined at the interface between the MC surface and the solution. For the gold-coated silicon MCs used in this work, $E = 168.5$ GPa, $t = 1$ μm , $L = 500$ μm , $\nu = 0.25$, and $s = 0.96$.

The surface stress generated by the interaction between guest **2** and the tetraphosphonate cavitant was determined to be equal to (-17 ± 2) mJ/m², while it was found to be (-12 ± 1) mJ/m² for the interaction with guests **1** and **3**. The stress was much lower for the interaction between the cavitant and guest **4**, (-2 ± 0.4) mJ/m².

From the above arguments, we conclude that MC deflection is directly related to $\Delta\sigma$, which in turn translates into the surface work driven by the host–guest complexation. At the molecular level, this work is very likely triggered by the interplay between host–guest complexation, cavitant desolvation, and interface adsorption, as also suggested by the order of magnitude of $\Delta\sigma$, which falls in the range of intermolecular forces.²⁷ Therefore, the ability of the cavitant functionalized MCs to discriminate mass differences as minute as a methyl group is due to the fact that the deflection response of the MCs to the cavitant–guest recognition event is related to the energy of the event rather than to the mass of the guest.

We recently framed analogous scenarios featuring biomolecular ligand–receptor interactions by implementing ad hoc thermodynamic models,^{7,28} but unfortunately none of them can be straightforwardly extended to the present system, mainly because of the differences between the biomolecule and the cavitant solid–solution interfacial phases and experimental conditions. Therefore, to support the interpretation of the relation between MC deflection and cavitant–guest recognition free energy, we investigated the thermodynamics of host–guest recognition in solution by ITC.

ITC Experiments. The complexation preferences of tetraphosphonate cavitants toward ammonium chloride guests **1–4** were independently assessed by ITC. In particular, direct as well as displacement binding experiments were performed to

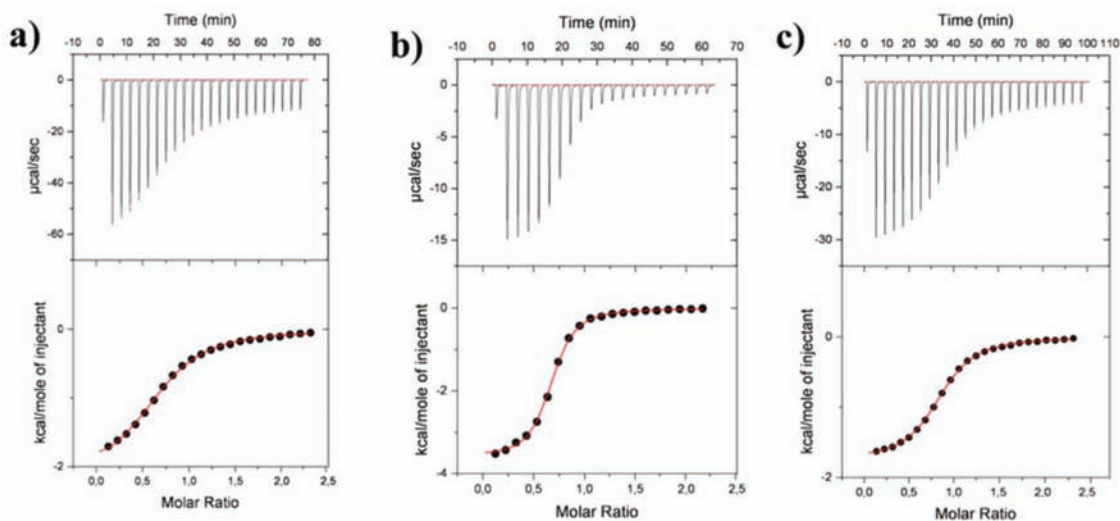


Figure 5. ITC data output of titrations in methanol at 303 K representing (a) the titration curve of guest 1, (b) that of guest 2, and (c) that of guest 3 into the host solution of cavitand $\text{Tiii}[C_3H_7, CH_3, Ph]$.

gain a quantitative thermodynamic picture of the host–guest interaction series.

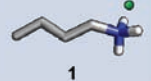

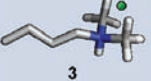
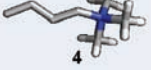
Representative titration data of the direct binding experiments between butylammonium (guest 1), *N*-methylbutylammonium (guest 2), and *N,N*-dimethylbutylammonium (guest 3) with cavitand $\text{Tiii}[C_3H_7, CH_3, Ph]$ are shown in Figure 5. Data for *N,N,N*-trimethylbutylammonium (guest 4) are not reported in Figure 5 as the interaction was too low to give significant titration signal. In the top panels of the figure, the downward peaks (heat pulses) represent the change in the feedback current associated with the consecutive injections of a small volume of guest solution into the ITC reaction cell containing a solution of $\text{Tiii}[C_3H_7, CH_3, Ph]$. The peak area is directly proportional to the enthalpy of guest binding. The differences in the magnitude of the peak intensities in the different panels are due the different choice in the host–guest concentration that was chosen case by case to obtain an optimal titration signal. The molarities were fixed at 4.5, 0.7, and 3.0 mM for the guests 1, 2, and 3, respectively.

After integration with respect to time and normalization per moles of added guest, the data were converted into the sigmoidal binding curves shown in the bottom panels of Figure 5, representing the normalized heat released from each injection against the molar ratio of the host and guest partners in the ITC cell.

Thermodynamic parameters of the host–guest interactions (the equilibrium constant K , and the changes in enthalpy, entropy, and free energy ΔH , ΔS , and ΔG) were extrapolated from the binding curves. The single-site (monovalent) model to fit the binding curve was adopted, supported by the crystal structure of a related $\text{Tiii}[H, CH_3, Ph] \cdot 2$ complex²⁰ and by the Job's plot titration of $\text{Tiii}[C_3H_7, CH_3, Ph]$ with the related sarcosine methyl ester hydrochloride guest (see Figure S1). As evidenced in Figure 5, this choice was nicely confirmed by the excellent agreement between the fit curve (continuous line) and the experimental points (●).

The determined K values are displayed in Figure 4B and summarized with the other thermodynamic parameters in Table 1. The strongest interaction is observed for complex $\text{Tiii}[C_3H_7, CH_3, Ph] \cdot 2$, with $K = (3.9 \pm 0.8) \times 10^5 \text{ M}^{-1}$. This

Table 1. Summary of ITC Measurements of the Titrations of the Guests 1–4 into the Solution of $\text{Tiii}[C_3H_7, CH_3, Ph]$ in Methanol at 303 K

Guest	$K \pm \delta K$ (M^{-1})	$\Delta H \pm \delta H$ ($\text{KJ} \cdot \text{mol}^{-1}$)	$\Delta G \pm \delta G$ ($\text{KJ} \cdot \text{mol}^{-1}$)	$T\Delta S \pm T\delta S$ ($\text{KJ} \cdot \text{mol}^{-1}$)
 1	$1.5 \pm 0.8 \cdot 10^3$	-8.7 ± 0.2	-18.5 ± 1.0	9.8 ± 1.7
 2	$3.9 \pm 0.8 \cdot 10^5$	-16.1 ± 0.6	-31.9 ± 0.5	15.8 ± 1.0
 3	$6.1 \pm 0.7 \cdot 10^3$	-8.7 ± 0.1	-22.0 ± 0.3	13.3 ± 0.5
 4	INTERACTION TOO LOW TO BE MEASURED			

preference is due to the synergistic activation of all three interaction modes available between 2 and the Tiii cavitand: (i) $CH_3-\pi$ interactions between the *N*- CH_3 moiety and the cavity of 1, (ii) cation–dipole interactions between the positively charged nitrogen and the $P=O$ dipoles, and (iii) the two concurrent hydrogen bonds between two adjacent $P=O$ on the upper rim of $\text{Tiii}[C_3H_7, CH_3, Ph]$ and the NH_2^+ unit.

The observed K values decrease about 2 orders of magnitude with guests 1 and 3. In the case of 3, the drop in binding strength is associated with the removal of one H-bond with the host, while for 1 it is imputable to the lack of $CH_3-\pi$ interactions. The two different interactions provide a comparable enthalpic contribution to the overall binding, with a slightly entropic gain in favor of $CH_3-\pi$ interactions.

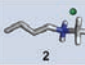





The ΔH and $T\Delta S$ results indicate that, in all three cases, the complexation is both enthalpy and entropy driven. The unusual entropic gain can be coarsely interpreted in terms of an increase

in solvent entropy associated with the desolvation (viz., solvent displacement) of both host and guest upon complexation.

Displacement binding experiments were performed to determine the affinity scale of the different guests toward cavitand $\text{Tiii}[C_3H_7, CH_3, Ph]$ under competitive conditions. This is of particular interest for future applications with low weight molecules with amino functionalities belonging to the biological and biomedical realms. To this aim, the effectiveness for specific binding to cavitand $\text{Tiii}[C_3H_7, CH_3, Ph]$ of the guest with higher K , **2**, in direct competition with the guests with lower K , **1** and **3**, was evaluated by displacement titration, following the procedures described in the Materials and Methods.

The results are summarized in Table 2 (see Figure S2 for ITC titration curves). Passing from entry I to entry II, a

Table 2. ITC Data Obtained from the Displacement Titrations, Using $\text{Tiii}[C_3H_7, CH_3, Ph]$ as Host^a

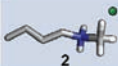

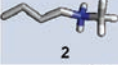

Entry	Guest	Host-guest complex	$K \pm \delta K$ (M^{-1})	$\Delta H \pm \delta H$ ($KJ \cdot mol^{-1}$)	ΔG ($KJ \cdot mol^{-1}$)	ΔS ($KJ \cdot mol^{-1}$)
I		$\text{Tiii}[C_3H_7, CH_3, Ph] \cdot 1$	$1.7 \pm 0.1 \cdot 10^4$	-13.1 ± 0.1	-24.6	11.5
Ia		$\text{Tiii}[C_3H_7, CH_3, Ph] \cdot 2$		NO exchange		
II		$\text{Tiii}[C_3H_7, CH_3, Ph] \cdot 3$	$5.3 \pm 0.2 \cdot 10^3$	-9.6 ± 0.1	-21.6	12.0
IIa		$\text{Tiii}[C_3H_7, CH_3, Ph] \cdot 2$		NO exchange		
III		$\text{Tiii}[C_3H_7, CH_3, Ph] \cdot 1$		Exchange, but not evaluable		
IIIa		$\text{Tiii}[C_3H_7, CH_3, Ph] \cdot 3$		NO exchange		

^aAll the experiments were performed in methanol.

decrease of one-half an order of magnitude of the displacement constant can be noticed. In both cases, we can observe a replacement of the prebound guests **1** and **3** with the strongest guest **2**, but in the second case the value is lower. This trend nicely agrees with that obtained from standard titrations: guest **1** has a weaker interaction with the host with respect to guest **3**. As a control experiment, the two reversed order titrations were also performed (see entries Ia and IIa of Table 2). In both cases, negligible power pulses were observed, meaning that no exchange occurred when the guests **1** and **3** were titrated in the preformed complex $\text{Tiii}[C_3H_7, CH_3, Ph] \cdot 2$. Finally, we directly checked guests **1** and **3** versus each other. As expected, the titration signal was too low to be significant. Results from these experiments resulted in agreement with the direct binding experiments when analyzed by the monoavalent competitive model (Table 3, see the Supporting Information for calculation details).²⁹

MC Experiments versus ITC Experiments. The comparison of Figure 4A and B evidences that MC deflections due to the complexation of the different guests with the immobilized cavitand follow a trend that fairly matches the trend of the complexation equilibrium constants in solution. Beyond the limits posed by comparing nonequilibrium and equilibrium data, this suggests that the MC deflection fairly mirrors the host-guest complexation free energy and in turn therefore qualitatively sorts the complexation properties of the host-guest partners. Work is in progress to implement MC

Table 3. Comparison of Calculated and Experimental K Values for the Displacement Titrations

Guest	Host-guest complex	$K \pm \delta K$ (M^{-1}) THEORETICAL	$K \pm \delta K$ (M^{-1}) EXPERIMENTAL
	$\text{Tiii}[C_3H_7, CH_3, Ph] \cdot 1$	$4.5 \pm 1.2 \cdot 10^4$	$1.7 \pm 0.1 \cdot 10^4$
	$\text{Tiii}[C_3H_7, CH_3, Ph] \cdot 2$	$5.8 \pm 1.6 \cdot 10^{-1}$	No exchange
	$\text{Tiii}[C_3H_7, CH_3, Ph] \cdot 3$	$1.2 \pm 0.6 \cdot 10^4$	$5.3 \pm 0.2 \cdot 10^3$
	$\text{Tiii}[C_3H_7, CH_3, Ph] \cdot 2$	2.7 ± 1.4	No exchange

experiments and develop a theoretical framework to relate solution and surface thermodynamics together with MC nanomechanical transduction.

Glycine versus Sarcosine Detection in Water. By shifting perspective, the discussion laid out above implies that the cavitand functionalized MCs can be deployed for screening LMW molecules bearing *N*-methylated moieties.

To benchmark this, the MCs were employed to assay sarcosine versus glycine, two amino acids that differ only for a *N*-methyl group. In addition, detection of sarcosine has an immediate biomedical impact, as its novel exploitation as a reliable marker for the early detection of prostate cancer is to date lively debated.^{2,30}

The experiments were run in water to match biological solvent conditions. Moreover, the direct comparison between glycine and sarcosine in methanol was not possible because glycine is insoluble in methanol. In water at neutral pH, both amino acids are in their zwitterionic forms.

Arrays of eight gold-coated MCs, functionalized with the active cavitand, were exposed to water solutions of sarcosine and glycine at a molar concentration of 1×10^{-4} M. The mean signal of the eight MCs was monitored during the flow of each guest through the microfluidic chamber. In Figure 6, each curve

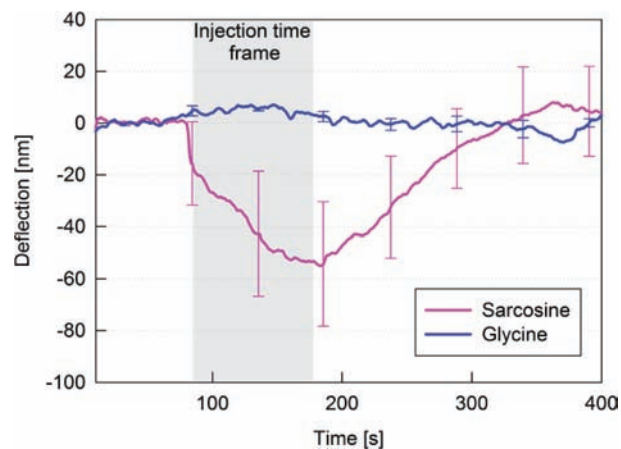


Figure 6. MC absolute deflection during the injection of 1×10^{-4} M sarcosine and glycine solutions in water (gray area). Each line represents the mean deflection of the eight MCs, and the error bars show the SD of the mean at selected points.

represents the mean deflection of the eight MCs, and the error bars show the SD of the mean at selected points when glycine

and sarcosine are injected into the chamber. The same procedure was used as for guests 1–4 except that pure water was used instead of methanol as solvent. The curves show a deflection of -55 nm when sarcosine is introduced in the chamber, while the MCs do not deflect when glycine flows, univocally indicating sarcosine detection and discrimination over glycine.

CONCLUSIONS

We showed that tetrakisphosphate cavitand functionalized MCs allow for real-time label-free selective screening across the *N*-methylammonium salt series. This is an unprecedented performance, if one considers that these LMW molecules weigh from 109 to 152 Da and differ from each other only by a few methyl groups (15 Da each).

The physicochemical origin of this outstanding selectivity was investigated by complementing MC experiments with ITC analysis of the thermodynamics of the host–guest interaction. It turned out that the MC deflection signal directly mirrors the host–guest complexation affinity. Therefore, the unique ability to sort LMW with mass differences as minute as a methyl group arises from the synergistic integration of the nanomechanical transduction mechanism of the MC with the complexation properties of the tetrakisphosphate cavitand. Work is in progress to perfect this picture by a tailored thermodynamic model.

This cavitand-MC platform was successfully benchmarked as a sensor by assaying sarcosine against glycine in aqueous solution. This result opens the route to applications in the “real” world and might immediately impact fundamental and applied research that needs screening of LMW compounds bearing *N*-methylated moieties, which range from drugs to cancer biomarkers and neurotransmitters.

ASSOCIATED CONTENT

Supporting Information

Additional information regarding the references, the synthesis methods for cavitands and guests, the ITC displacement titrations, the calculations of the apparent binding affinities, the NMR spectra of cavitands and guests, and the ^{31}P NMR Job plot of the complex **Tiiii-sarcosine methyl ester**. This material is available free of charge via the Internet at <http://pubs.acs.org>.

AUTHOR INFORMATION

Corresponding Author

paolo.bergese@ing.unibs.it; enrico.dalcanale@unipr.it

ACKNOWLEDGMENTS

This work was funded by the grant Nanomechanical Sensors for Anfetamins (SNAF) (Regione Lombardia-INSTM), by Fondazione CARIPARMA through the project SpA, and by the German-Italian exchange Program (Vigoni Program).

REFERENCES

- (1) ATLAS on Substance Use (2010) – Resources for the prevention and treatment of substance use disorders; World Health Organization, 2011.
- (2) Sreekumar, A.; et al. *Nature* **2009**, *457*, 910–914.
- (3) Von Bohlen und Halbach, O.; Dermietzel, R. *Neurotransmitters and Neuromodulators: Handbook of Receptors and Biological Effects*; Wiley-VCH: Weinheim, 2006.
- (4) Bosker, W. M.; Huestis, M. A. *Clin. Chem. (Washington, DC, U.S.)* **2009**, *55*, 1910–1931.

- (5) (a) Soares, M. E.; Carvalho, F.; Bastos, M. L. *Biomed. Chromatogr.* **2001**, *15*, 452–456. (b) Fang, C.; Chung, Y.-L.; Liu, J.-T.; Lin, C.-H. *Forensic Sci. Int.* **2002**, *125*, 142–148. (c) Butler, D.; Pravda, M.; Guilbault, G. *Anal. Chim. Acta* **2006**, *556*, 333–339.
- (6) Bergese, P.; Cretich, M.; Oldani, C.; Oliviero, G.; Di Carlo, G.; Depero, L. E.; Chiari, M. *Curr. Med. Chem.* **2008**, *15*, 1706–1719.
- (7) (a) Bergese, P.; Oliviero, G.; Alessandri, I.; Depero, L. E. *J. Colloid Interface Sci.* **2007**, *316*, 1017–1022. (b) Federici, S.; Oliviero, G.; Hamad-schifferli, K.; Bergese, P. *Nanoscale* **2010**, *2*, 2570–2574. (c) Oliviero, G.; Federici, S.; Colombi, P.; Bergese, P. *J. Mol. Recognit.* **2011**, *24*, 182–187.
- (8) Arlett, J. L.; Myers, E. B.; Roukes, M. L. *Nat. Nanotechnol.* **2011**, *6*, 203–215.
- (9) Fritz, J. *Analyst* **2008**, *133*, 855–863.
- (10) (a) Bergese, P.; Oliviero, G.; Colombo, I.; Depero, L. E. *Langmuir* **2009**, *2*, 9–11. (b) Oliviero, G.; Maiolo, D.; Leali, D.; Federici, S.; Depero, L. E.; Presta, M.; Mitola, S.; Bergese, P. *Biosens. Bioelectron.* **2010**, *26*, 1571–1575.
- (11) Kang, K.; Sachan, A.; Nilsen-Hamilton, M.; Shrotriya, P. *Langmuir* **2011**, *27*, 14696–14702.
- (12) Sepaniak, M.; Datskos, P.; Lavrik, N.; Tipple, C. *Anal. Chem.* **2002**, *74*, S68–S75A.
- (13) (a) Dutasta, J.-P. *Top. Curr. Chem.* **2004**, *232*, 55–91. (b) Pinalli, R.; Suman, M.; Dalcanale, E. *Eur. J. Org. Chem.* **2004**, 451–462. (c) Nifantsev, E. E.; Maslennikova, V. I.; Merkulov, R. V. *Acc. Chem. Res.* **2005**, *38*, 108–116.
- (14) Melegari, M.; Suman, M.; Pirondini, L.; Moiani, D.; Massera, C.; Ugozzoli, F.; Kalenius, E.; Vainiotalo, P.; Mulatier, J.-C.; Dutasta, J.-P.; Dalcanale, E. *Chem.-Eur. J.* **2008**, *14*, 5772–5779.
- (15) (a) Yebeutchou, R. M.; Tancini, F.; Demitri, N.; Geremia, S.; Mendichi, R.; Dalcanale, E. *Angew. Chem., Int. Ed.* **2008**, *47*, 4504–4508. (b) Tancini, F.; Yebeutchou, R. M.; Pirondini, L.; De Zorzi, R.; Geremia, S.; Scherman, O. A.; Dalcanale, E. *Chem.-Eur. J.* **2010**, *16*, 14313–14321.
- (16) Tancini, F.; Genovese, D.; Montalti, M.; Cristofolini, L.; Nasi, L.; Prodi, L.; Dalcanale, E. *J. Am. Chem. Soc.* **2010**, *132*, 4781–4789.
- (17) Yebeutchou, R. M.; Dalcanale, E. *J. Am. Chem. Soc.* **2009**, *131*, 2452–2453.
- (18) Kalenius, E.; Moiani, D.; Dalcanale, E.; Vainiotalo, P. *Chem. Commun.* **2007**, 3865–3867.
- (19) Biavardi, E.; Battistini, G.; Montalti, M.; Yebeutchou, R. M.; Prodi, L.; Dalcanale, E. *Chem. Commun.* **2008**, 1638–1640.
- (20) Biavardi, E.; Favazza, M.; Motta, A.; Fragalà, I. L.; Massera, C.; Prodi, L.; Montalti, M.; Melegari, M.; Condorelli, G. G.; Dalcanale, E. *J. Am. Chem. Soc.* **2009**, *131*, 7447–7455.
- (21) Schmidtchen, F. P. Isothermal Titration Calorimetry in Supramolecular Chemistry. In *Analytical Methods in Supramolecular Chemistry*; Schalley, C. A., Ed.; Wiley-VCH: Weinheim, 2007; pp 55–78.
- (22) Velazquez-Campoy, A.; Freire, E. *Nat. Protoc.* **2006**, *1*, 186–191.
- (23) Dionisio, M.; Maffei, F.; Rampazzo, E.; Prodi, L.; Pucci, A.; Ruggeri, G.; Dalcanale, E. *Chem. Commun.* **2011**, 6596–6598.
- (24) Wei, A. *Chem. Commun.* **2006**, 1581–1591.
- (25) For the sensing properties of SAMs of MeCav, see: Schierbaum, K. D.; Weiss, T.; van Velzen, E. U.; Engbersen, J. F.; Reinhoudt, D. N.; Gopel, W. *Science* **1994**, *265*, 1413–1415.
- (26) Evans, D. R.; Craig, V. S. J. *J. Phys. Chem. B* **2006**, *110*, 19507–19514.
- (27) Israelachvili, J. N. *Intermolecular and Surface Forces, with Applications to Colloidal and Biological Systems*; Academic Press: London, 1985.
- (28) De Puig, H.; Federici, S.; Baxamusa, S. H.; Bergese, P.; Hamad-Schifferli, K. *Small* **2011**, *7*, 2477–2484.
- (29) Haynie, D. T. *Biological Thermodynamics*; Cambridge University Press: Cambridge, 2008.
- (30) Schalken, J. A. *Eur. Urol.* **2010**, *58*, 19–21.